International Journal of Innovative Computing, Information and Control
Volume **8**, Number **2**, February **2012**
 ISSN 1349-4198
pp. 1025–1036

DESIGN AND IMPLEMENTATION OF A HIGH PERFORMANCE HARD DISK DRIVE SERVO CONTROLLER USING GA BASED 2DOF ROBUST CONTROLLER

Somyot Kaitwanidvilai[1] and Amar Nath[2]

[1]Faculty of Engineering
[2]College of Data Storage Innovation
King Mongkut's Institute of Technology Ladkrabang
Chalongkrung Rd., Ladkrabang, Bangkok 10520, Thailand
drsomyotk@gmail.ac.th; kksomyot@kmitl.ac.th; amar_2102@hotmail.com

Received August 2010; revised December 2010

Abstract. *Currently, HDD (Hard Disk Drive) with VCM actuator covers more than 80% of the HDD market. To enhance the capacity and ability of the system, a new class of servo controller is required to achieve both the robustness and performance of the entire system. This paper proposes a new technique for designing a robust controller for HDD with Voice Coil motor (VCM) actuator; the control design problem, H_∞ loop shaping with structured controller, is solved by Genetic Algorithm (GA). The proposed technique does not only solve the problem of high order controller in the conventional design, but also still retains the robust performance of conventional H_∞ control technique. In addition, structured pre-filter in the 2DOF control scheme is also designed by GA to enhance the performance in terms of time-domain tracking. Simulation and experimental results verify the effectiveness of our proposed technique.*
Keywords: HDD servo system, Robust control, H_∞ loop shaping, Genetic algorithm

1. **Introduction.** The trend in hard disk design is of smaller hard disk with larger capacity. The recording density is increasing at an impressive annual rate of more than 40% while the access time is decreasing; very soon, the storage density is going to cross one terra-bit per square inch [1]. The expected necessary track density for 1 terra-bit per square inch recording will be 500,000 tracks-per-inch (TPI), which requires a TMR budget of less than 5nm (3-sigma value) [1]. The existing conventional HDD servo technologies cannot support this new requirement; a new class of VCM actuator (or Dual Stage Actuator) along with a high performance servo controller is required to handle both the performance and robustness.

As the TPI increases, the track width becomes narrow, which leads to lower tolerance in the positioning of the head. The controller for track following has to achieve tighter regulation in the control of servo mechanism. A rigorous analysis of the sources of position error (PES) and the development of advanced techniques to eliminate the effect of these sources are required. Currently, HDD uses several control techniques such as lead lag compensators, PI compensators, robust control and notch filters; however, some classical methods for controlling HDD servo can no longer meet the demand of higher performance. Several control approaches have been adopted to solve the above mentioned problem, e.g., the identification and the high bandwidth control [2], the mixed H_2/H_∞ Control for improving TMR [3], the dynamic nonlinear control for fast seek-settling [4] and the gradient based parameter optimization method [5]. However, the problems of high order of the resulting controller and the complicated design procedure are still the main problems of the above mentioned approaches. In addition, since the performance of the servo controllers are governed by the mechanical repeatable run out (RRO) and non repeatable run-out (NRRO), a lot of research works have been done to improve the RRO/NRRO and the servo performance, e.g., Western Digital Inc US patents documents US7616399 [6]; this invention preserves the PES continuity during track following mode. Western Digital Inc US patents documents US6585435 [7] describes a method of RRO learning before and after shipping to cancel the RRO in a disk drive.

In this paper, we propose a new class of controller which contains the same degree of robustness as H_∞ robust controller; at the same time, its controller order is much lower than that of the conventional controller. We utilize the Genetic Algorithm (GA) to design this controller. The remainder of this paper is organized as follows: Section 2 describes an overview of HDD servo system and the dynamic model; Section 3 illustrates the conventional H_∞ loop shaping design technique; the proposed technique, Genetic Algorithm (GA) based fixed-structure robust controller, is described in Section 4, Section 5 shows the simulation and experimental results; and Section 6 concludes the paper.

2. **Overview.** HDD servo system needs to carry out two main tasks; first is to move the head to the desired track as quickly as possible, and then position the head on the center of the track as precisely as possible so that data can be read/written quickly and reliably. The first task is commonly referred to as *track seeking*, while the second task is *track following* [1]. The mechanical components of HDD include a VCM, a suspension and a slider as shown in Figure 1.

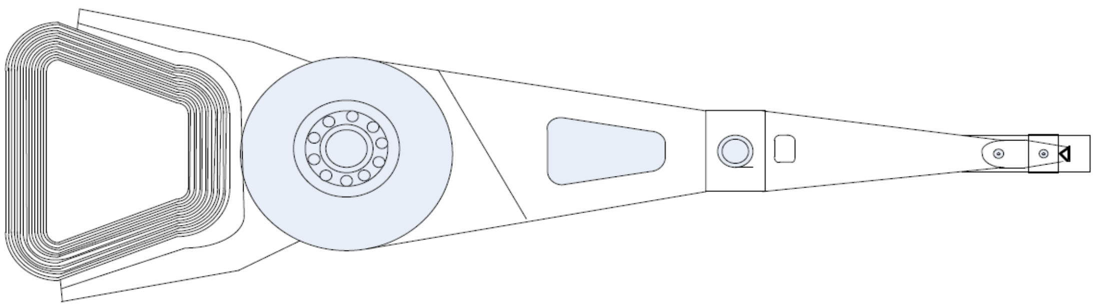

Figure 1. Example of VCM actuator

As seen in this figure, read/write head is fabricated on the edge of slider. The slider is supported by the suspension and flies over the surface of disk on an air-bearing surface (ABS). Dynamic model of HDD servo system can be characterized as a double integrator cascaded with several high frequency resonance modes. The dynamic model of an ideal VCM actuator can be formulated as a second order state space model as the following equation [10].

$$\begin{pmatrix} \dot{y} \\ \dot{v} \end{pmatrix} = \begin{bmatrix} 0 & k_y \\ 0 & 0 \end{bmatrix} \begin{pmatrix} y \\ v \end{pmatrix} + \begin{pmatrix} 0 \\ k_v \end{pmatrix} u \tag{1}$$

where u is the actuator input (volt); y and v are the position (track) and the velocity of the R/W head; K_y is the position measurement gain; $K_y = \dfrac{K_t}{m}$; K_t is the current/force conversion coefficient and m is the mass of the VCM actuator. Consequently, the transfer function of an ideal VCM actuator model can be written as a double integrator transfer function. However, if the high-frequency resonance modes are considered, a more realistic model for the VCM actuator will be [10]:

$$G_v(s) = \frac{k_v k_y}{s^2} \prod_{i=1}^{N} G_{r,i}(s) \tag{2}$$

where

$$G_{r,i}(s) = \frac{a_i s^2 + b_i s + \omega_i^2}{s^2 + 2\xi_i \omega_i s + \omega_i^2} \tag{3}$$

N is the number of resonance modes; $G_{r,i}(s)$ is the i^{th} resonance mode term. a_i, b_i, ξ_i and ω_i are the coefficients of i^{th} resonance mode dynamic. In this paper, a HDD servo system with the model shown in Table 1 is studied [10,11].

Table 1. VCM parameters with tolerances

Parameter	Value	Tolerance
M	2 Kg	–
k_t	20	–
k_v	6.4013×10^5	–
ω_1	$2\pi 1905$	3%
ω_2	$2\pi 2511$	5%
ω_3	$2\pi 5011$	5%
ω_4	$2\pi 8317$	5%
ξ_1	0.015	10%
ξ_2, ξ_3, ξ_4	0.025	10%
a_1	0.912	–
a_2	0.7286	–
b_1	457.4	–
b_2	962.2	–

As seen in Table 1, the VCM actuator has four resonance modes at the resonance frequencies of 1095, 2511, 5011 and 8817 Hz. In order to reduce the effect of high frequency resonance mode, notch filter is added. The notch filter can be modeled using Equations (4) and (5). For example, three notch filters described in Table 2 have been used to compensate the plant resonances.

$$N_r(s) = \prod_{i=1}^{N} N_{n,i}(s) \tag{4}$$

where

$$N_{r,i}(s) = \frac{s^2 + 2\xi_{ni}\omega_{ni} s + \omega_{ni}^2}{s^2 + 2\xi_{ni+1}\omega_{ni} s + \omega_{ni}^2} \tag{5}$$

Table 2. VCM notch parameters

Notch	ξ_{ni}	ξ_{ni+1}	ω_{ni}
1	0.01	0.10	$2.\pi.1900$
2	0.01	0.10	$2.\pi.2500$
3	0.01	0.20	$2.\pi.5000$

By Equations (2) and (3), the plant can be derived as 10^{th} order transfer function as given in Equation (6), and by Equations (4) and (5), we can obtain the notch filter model as Equation (7).

$$Plant = \left\{ \frac{1.197 \times 10^{26}s^4 + 2.12 \times 10^{29}s^3 + 5.826 \times 10^{34}s^2 + 4.366 \times 10^{37}s + 6.189 \times 10^{42}}{\begin{array}{l} s^{10} + 5336s^9 + 4.124 \times 10^9 s^8 + 1.302 \times 10^{13}s^7 + 4.216 \times 10^{18}s^6 + 6.72 \times 10^{21}s^5 + 1.198 \times 10^{27}s^4 \\ +7.946 \times 10^{29}s^3 + 9.668 \times 10^{34}s^2 \end{array}} \right\} \tag{6}$$

$$Notch = \left\{ \frac{s^6 + 1181s^5 + 1.377 \times 10^9 s^4 + 8.94 \times 10^{11}s^3 + 4.194 \times 10^{17}s^2 + 1.244 \times 10^{20}s + 3.47 \times 10^{25}}{s^6 + 18100s^5 + 1.453 \times 10^9 s^4 + 1.14810^{13}s^3 + 4.397 \times 10^{17}s^2 + 1.465 \times 10^{21}s + 3.47 \times 10^{25}} \right\} \tag{7}$$

Position error signal (PES) is an essential feedback signal for servo control system during the track following operation. The PES signal may be derived from the servo burst of the servo sector of the disk. The performance of track-following servo system is normally measured by an index, track mis-registration (TMR), which is an index used to measure the variance of the deviation between the center of the read/write head and the center of the track.

3. **Conventional $\mathbf{H_\infty}$ Loop Shaping.** This approach requires two weighting functions, W_1 (pre-compensator) and W_2 (post-compensator), for shaping the nominal plant G_0 so that the desired open loop shape is achieved. In this approach, the shaped plant is formulated as normalized co-prime factor, which separates the shaped plant G_s into normalized co-prime factors N_S and M_s [9]. Note that,

$$G_s = W_1 G_0 W_2 = M_s N_s^{-1} \tag{8}$$

The following steps briefly describe the procedure of H_∞ loop shaping controller design.

Step 1: Shape the singular values of the nominal plant G_0 by a pre-compensator W_1 and/or a post-compensator W_2 to get the desired loop shape. In SISO system, the weighting functions W_1 and W_2 can be chosen as:

$$W_1 = K_W \frac{s+a}{s+b} \quad W_2 = \frac{s+c}{s+d} \tag{9}$$

where a, b, K_W, c and d are positive numbers. The perturbed plant of the shaped plant (Figure 2) can be written as:

$$G_\Delta = (N_s + \Delta_{Ns})(M_s + \Delta_{Ms})^{-1} \tag{10}$$

where Δ_{Ns} and Δ_{Ms} are the uncertainty transfer functions of nominator and denominator, and $\|\Delta_{Ns}, \Delta_{Ms}\| \leq \varepsilon$, ε is the uncertainty boundary called stability margin.

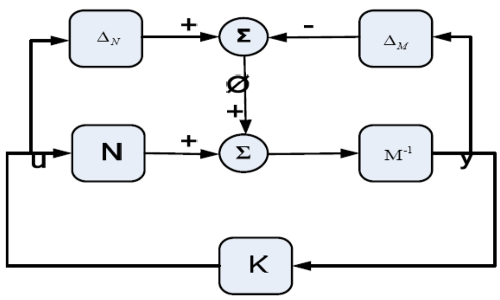

FIGURE 2. Normalize co-prime factor uncertainty [9]

Step 2: Calculate ε_{opt} by solving the following inequality:

$$\gamma_{opt} = \varepsilon_{opt}^{-1} = \inf_{stab\ K} \left\| \begin{bmatrix} I \\ K \end{bmatrix} (I + GK)^{-1} M_s^{-1} \right\| \tag{11}$$

To determine ε_{opt}, there is a unique method as follows:

$$\gamma_{\min} = \varepsilon_{\max}^{-1} = (1 + \lambda_{\max}(X.Z))^{1/2} \tag{12}$$

where Z and X are the solutions of two Riccati equations in Equations (13) and (14) respectively, $\lambda_{\max}$ is denoted as the maximum eigen-value. A, B, C and D represent the state space matrices of the shaped plant.

$$\left(A - BS^{-1}D^TC\right)Z + Z\left(A - BS^{-1}D^TC\right)^T - ZC^TR^{-1}CZ + BS^{-1}B^T = 0 \tag{13}$$

$$\left(A - BS^{-1}D^TC\right)X + X\left(A - BS^{-1}D^TC\right)^T - XBS^{-1}B^TX + C^TR^{-1}C = 0 \tag{14}$$

where

$$S = I + D^TD$$
$$R = I + DD^T$$

If ε_{opt} is not satisfied (too low), then go to Step 1 to adjust the weighting functions [9].

Step 3: Select $\varepsilon < \varepsilon_{opt}$ and then synthesize a controller K_∞ that satisfies Equation (15)

$$\left\| \begin{bmatrix} I \\ K_\infty \end{bmatrix} (I + G_\infty K_\infty)^{-1} M_s^{-1} \right\| \le \varepsilon^{-1} \tag{15}$$

Controller K_∞ is obtained by solving the sub-optimal control problem in Equation (15). The details of this solving are shown in [9].

Step 4: Final controller (K_∞) is determined by:

$$K = W_1 K_\infty W_2 \tag{16}$$

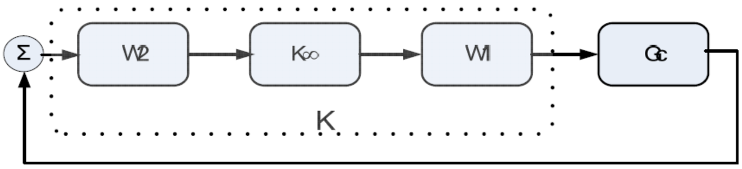

FIGURE 3. H_∞ loop shaping controller [9]

4. **GA Based Fixed-structure H_∞ Loop Shaping Optimization.** One of the most important aspects in HDD servo control is to ensure both the stability and the performance of the system under the perturbed conditions. One of the most popular techniques used for achieving this task is H_∞ loop shaping control. In this technique, the uncertainty and performance are incorporated into the controller design [8,9]. Unfortunately, the order of the resulting controller from this technique is usually high, which makes it difficult to implement in practice. In this paper, we illustrate the design of a HDD controller which can guarantee stability under the perturbed conditions, and which also has a simple structure. This paper uses a more recent evolutionary technique, Genetic Algorithms (GA), to solve the fixed-structure H_∞ loop shaping optimization problem. Infinity norm of transfer function from disturbances to states is formulated as a cost function in our optimization problem [8,15,16]. The resulting optimal controller makes the system stable and also guarantees the robust performance. In addition, GA is adopted to find a structured pre-filter for increasing the tracking performance of the system. By the approach mentioned above, a high performance HDD servo system can be designed.

Genetic algorithms are well known as a biologically inspired class of algorithms applicable to any nonlinear optimization problem. It has been used in many kinds of applications, for example, classification learning [12], robust optimal PID controller [13], airline crew scheduling [14]. This algorithm applies the concept of chromosomes, and the genetic operations of crossover, mutation and reproduction. A chromosome is an individual sample in a population; each individual is assigned a fitness based on the specified fitness function. At each step, called generation, fitness values of all individuals in a population are calculated. Individual with maximum fitness value is retained as a solution in the current generation. To form a new population, genetic operators, i.e., crossover, mutation and reproduction are adopted. More information about GA can be seen in [8,15].

Although the proposed controller is structured, it still retains the entire robustness and performance guarantee as long as a stability margin ε is achieved. The proposed optimization goal is to find the parameter p in controller $K(p)$ that minimizes infinity norm from disturbances w to states z, $\|T_{ZW}\|_\infty$. From Equation (16), assuming that W_1 and W_2 are invertible, then $K_\infty = W_1^{-1}K(p)W_2^{-1}$. Substituting this equation into Equation (15), the ∞-norm of the transfer function matrix $\|T_{ZW}\|_\infty$ which is subjected to be minimized can be written as:

$$J_{\text{cost}} = \gamma = \|T_{ZW}\|_\infty = \left\| \begin{bmatrix} I \\ W_1^{-1}K(p)W_2^{-1} \end{bmatrix} \left(I + G_s W_1^{-1}K(p)W_2^{-1}\right)^{-1} M_s^{-1} \right\|_\infty \tag{17}$$

The optimization problem can be written as:

$$\text{Minimize} \left\| \begin{bmatrix} I \\ W_1^{-1}K(p)W_2^{-1} \end{bmatrix} \left(I + G_s W_1^{-1}K(p)W_2^{-1}\right)^{-1} M_s^{-1} \right\|_\infty$$

Subject to $p_{i,\min} < p_i < p_{i,\max}$, where $p_{i,\min i}$ and $p_{i,\max}$ are lower and upper bounds of parameter p_i in controller $K(p)$, respectively. The fitness function in the controller synthesis can be written as the following equation.

$$Fitness = \left\{ \begin{array}{l} \left(\left\| \begin{bmatrix} I \\ W_1^{-1}K(p)W_2^{-1} \end{bmatrix} \left(I + G_s W_1^{-1}K(p)W_2^{-1}\right)^{-1} M_s^{-1} \right\|_\infty \right)^{-1} \\ \qquad\qquad \text{If } K(p) \text{ stabilizes the plant.} \\ 0.00001 \quad \text{Otherwise.} \end{array} \right\} \tag{18}$$

The fitness is set to a small value (in this case is 0.00001) if $K(p)$ does not stabilize the plant.

5. Simulation and Experimental Results.

5.1. The proposed design.

According to the bode stability criteria, the typical bode magnitude plot of the open loop transfer function of a compensated plant should have the following characteristics [17,18].

1. The bode magnitude plot of the compensated plant should have a high gain above 0 dB at low frequency and decreases with increasing frequency at a rate of $-20*$N dB/decade, where N is an integer and N > 2.
2. The bode magnitude plot of the compensated plant crosses the 0 dB with a slope of approximately -20 dB/decade to ensure the stability.
3. The bode magnitude plot of the compensated plant should have low gain under 0 dB and decreases with increasing frequency at a rate of $-20*$N dB/decade (N > 2).

In addition, the following specifications are needed for the designed system [19]:

1) Overshoot and undershoot of the step response should be kept less than 5% as the read/write head can start to read or write within 5% of the target.
2) The 5% settling time in the step response should be less than 2 ms.

In our study, the plant is shown in Equation (6) and the designed notch filter is shown in Equation (7). Based on the above mentioned specifications and guidelines [9]; the weights W_1 and W_2 can be selected as:

$$W_1 = 4.99 * \frac{s + 617.41}{s + 1.09} \quad W_2 = \frac{s + 81.23}{s + 130470} \tag{19}$$

By these weights, a gain margin of 12 dB and a phase margin of 67.5° can be achieved. First, we applied the conventional H_∞ loop shaping (HLS) technique to design a robust controller. The resulting controller by this approach is 18^{th} order robust controller, and it can achieve the robust performance with $\gamma = 1.7723$. However, the order of HLS controller is 18 and it is not easy to implement practically.

Next, a fixed-structure robust controller using the proposed algorithm is designed. The structure of controller is selected as the second order lead-lag controller which can be expressed in Equation (20).

$$Cont = k_3 \frac{(s + k_1)(s + k_2)}{(s + k_4)(s + k_5)} \tag{20}$$

In the optimization, the ranges of controller parameters and GA parameters are set as follows. By considering W_1 and W_2, the ranges of controller parameters can be selected as: $k_1 \in [10\ 100]$; $k_2 = [500\ 1500]$; $k_3 \in [1\ 10]$; $k_4 \in [0.01\ 10]$ and $k_5 \in [10000\ 150000]$. Population size = 100; crossover probability = 0.6; mutation probability = 0.1 and maximum generation = 30. When running GA for 14 generations, an optimal controller can be found as:

$$Cont(PPD) = 4.7787 \frac{(s + 51.87)(s + 689.89)}{(s + 0.4879)(s + 134600)} \tag{21}$$

Figure 4 shows a plot of the convergence of the fitness values (stability margin) versus generations. As shown in this figure, the optimal robust controller provides a satisfied stability margin at 0.5156.

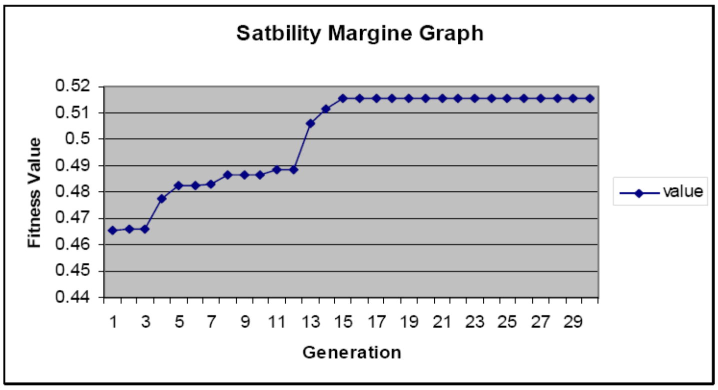

Figure 4. Convergence of the fitness values

Figure 5 shows the comparison of the shaped plant by the proposed controller and HLS. In this figure, the HLS controller is able to provide gain margin of 13.4 dB with phase margin of 65.3°, while the proposed GA based controller without pre-filter is able to provide gain margin of 12.6 dB and phase margin of 66.1°.

5.2. **The pre-compensator for improving tracking performance.** In addition, we designed a fixed-structure pre-filter to achieve the tracking performance specification.

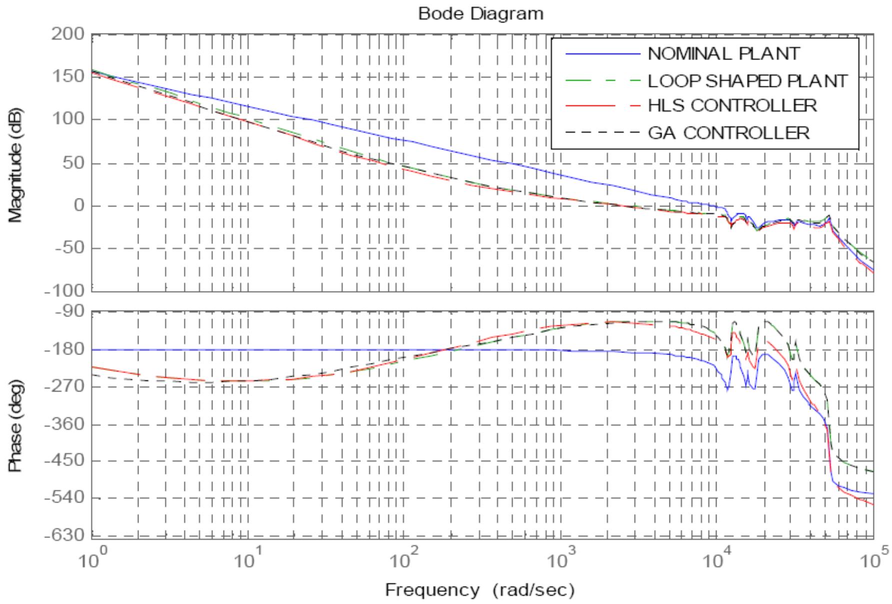

FIGURE 5. Bode diagrams of the open loop transfer function of the shaped plant, nominal plant, plant with HLS and the proposed controllers

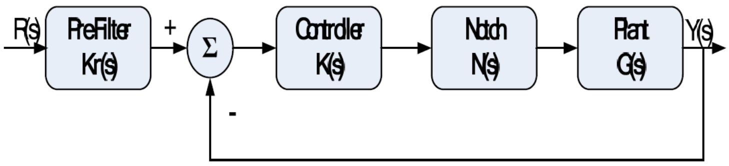

FIGURE 6. 2DOF control system

Figure 6 shows the structure of 2DOF control adopted in our design. In the pre-filter, we selected a 1st order lead-lag controller, $K_r(s)$ as [9]:

$$K_r(s) = \frac{\tau_{lead}s + 1}{\tau_{lag}s + 1} \tag{22}$$

In our optimization problem, the constraints are set as follows: over shoot <= 5%, and 5% settling time <= 1.5 ms. For the pre-filter, the parameters attempted to be evaluated are time constants, τ_{lead} and τ_{lag}. By running GA, we found that the optimal $K_r(s)$ is.

$$K_r(s) = \frac{0.001671s + 1}{0.002122s + 1} \tag{23}$$

Responses from the unit step commands by HLS and the proposed robust controller at the nominal plant are shown in Figure 9. Table 3 shows the performance obtained by the controllers. As seen in this figure and Table 3, the maximum overshoot obtained by the (1 DOF) HLS controller is much higher than that of the proposed 2DOF controller. Moreover, 5% settling time of the proposed controller is much faster than that of the conventional HLS controller. Clearly, time domain specifications can be achieved by the proposed technique.

5.3. **Robustness test.** For testing the robustness of the designed system, the resonance mode frequencies $(\omega_1, \omega_2, \omega_3, \omega_4)$ and damping coefficients $(\xi_1, \xi_2, \xi_3, \xi_4)$ of the system have been changed to the values specified in Table 4. We performed our robustness test using MATLAB robustness stability utility [21] by changing the plant parameters according to

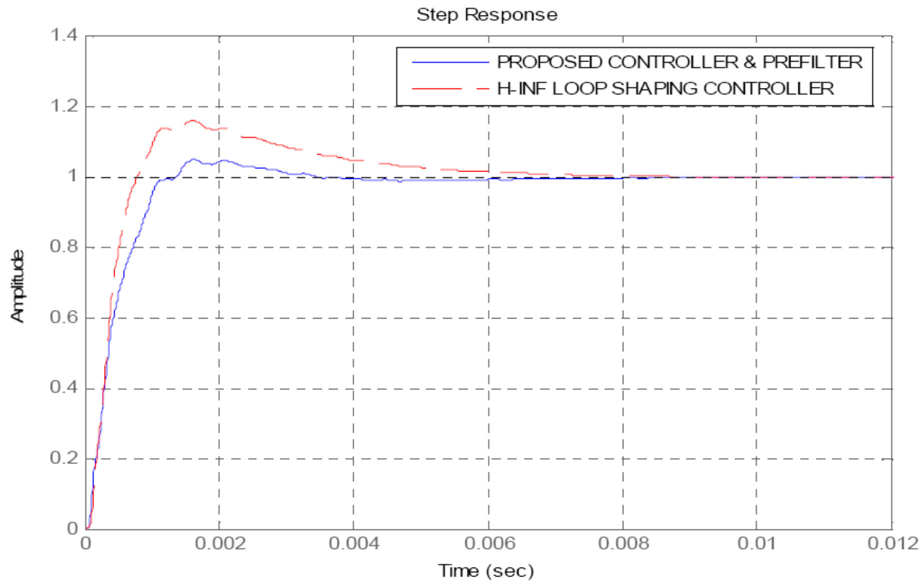

FIGURE 7. Step response from the HLS and the proposed controller

TABLE 3. Performance comparison table

Controller	Conventional PID	HLS	The proposed controller
Order	2	18	2 (with 1 pre-filter)
Over shoot	18.6%	15.8%	4.9%
Settling time	3.36 ms	3.89 ms	0.96 ms
Rise time	0.47 ms	0.48 ms	0.80 ms

Table 4. The open loop bode, step response and stability robustness under closed loop system have been analyzed.

TABLE 4. Parameters uncertainty table

Parameter	*Nominal Value*	*Uncertainty Tolerance*
ω_1	6880.1	$+/-3\%$
ω_2	15777	$+/-5\%$
ω_3	31845	$+/-5\%$
ω_4	52257	$+/-5\%$
ξ_1	0.015	$+/-10\%$
ξ_2, ξ_3, ξ_4	0.025	$+/-10\%$

Open loop bode for nominal and uncertain system and is given in Figure 8(a). As seen in this figure, our nominal and uncertain plots are almost the same even during uncertain zone. They lay within a few dB variations around the nominal plant. Figure 8(b) shows the step responses of the proposed controllers under the perturbed conditions. This figure shows that the proposed controller can provide the satisfied responses even the parameters of the system are changed.

In order to verify the proposed technique, we implemented our technique to design a controller in real HDD servo system with single stage VCM actuator. Figure 9 shows our experimental setup.

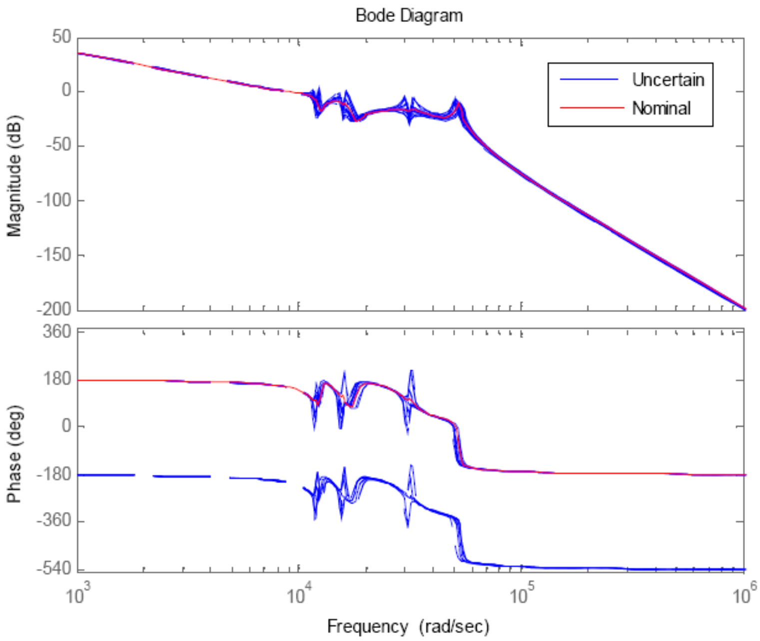

(a)

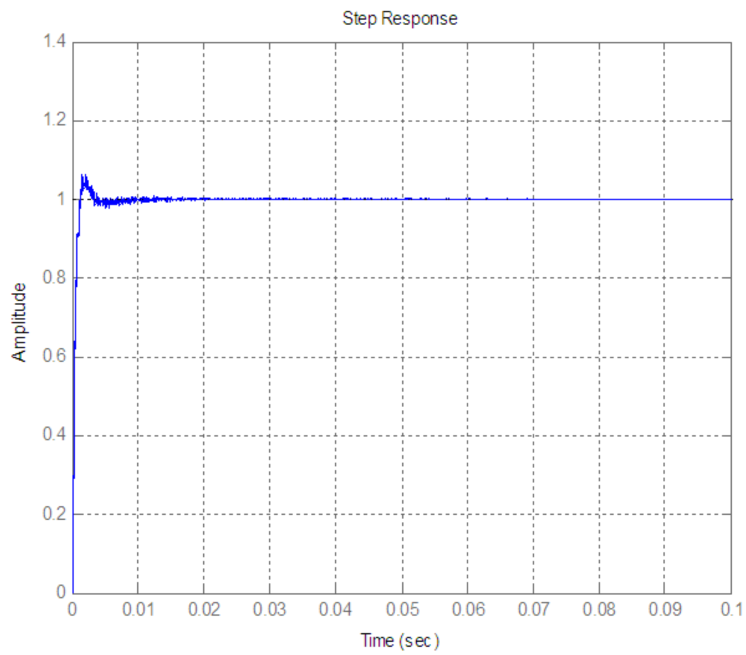

(b)

FIGURE 8. (a) Frequency domain and (b) time domain responses of the plant under perturbed and normal conditions

The controller was implemented on firmware (F/W). The graphical user interface (GUI) is used to download the F/W on HDD and to command the input, e.g., perform seek. MATLAB scripts were used for analysis and to plot the data. We implemented our technique on the actual HDD which plant and notch filter are different from those in

Figure 9. Experimental setup

the simulation study. The plant and notch filters are proprietary to company; thus, we cannot disclose our implemented plant. In our experiments, the real plant is adapted in our design along with Adaptive Feed Forward compensator (AFC). The AFC is used to compensate $1\times$ and $2\times$ RRO components. The experimental results are shown in Figure 10. As seen in this figure, our proposed controller along with AFC is able to work well within 14.8% of the track width. Figure 10(a) shows the deviation of PES signal; the max and min lines describe the maximum deviation (in positive and negative directions) between the position of head and the center of target track. From Figure 10, we can see that our proposed system can perform well within $+/-20$ nm. The histogram was plotted based on 4K (4096) samples. Based on these samples, we can see that over 84% of the total samples (3450 samples) were controlled well within $+/-10$ nm.

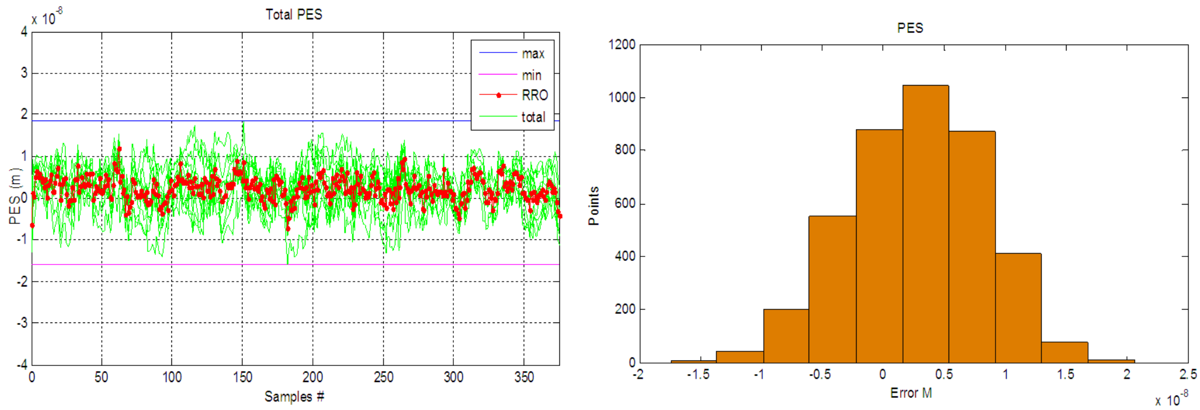

(a) (b)

Figure 10. (a) The PES on track with the proposed controller and (b) the histogram of the PES error

6. **Conclusions.** In this paper, the design of a high-performance and robust controller for HDD servo system using Genetic Algorithm has been proposed. Results show that the response from our proposed technique has significantly lower overshoot compared with that of the conventional PID and HLS. In addition, the order of controller is much lower than that of the HLS controller, but the robust performance from the proposed controller is almost the same as HLS. The tracking performance specifications can be achieved by the proposed controller. Implementation on a HDD servo system verifies the effectiveness of the proposed controller.

Acknowledgement. This work was funded by DSTAR, KMITL and NECTEC, NSTDA (under Grant No. DSTARR & D 02-03-52).

REFERENCES

[1] X. Huang, R. Nagamune and R. Horowitz, A comparison of multi rate robust track-following control synthesis techniques for dual-stage and multi sensing servo systems in hard disk drives, *IEEE Trans. on Magnatics*, vol.42, no.7, pp.1896-1904, 2006.

[2] P. A. Ioannou, H. Xu and B. Fidan, Identification and high bandwidth control of hard disk drive servo systems based on sampled data measurements, *IEEE Trans. on Control Systems Technology*, vol.15, no.6, pp.1089-1095, 2007.

[3] C. Du, L. Xie, J. N. Teoh and G. Guo, An improved mixed H2/H∞ control design for hard disk drives, *IEEE Trans. on Control Systems Technology*, vol.13, no.5, pp.832-839, 2005.

[4] Y. Li, V. Venkataramanan, G. Guo and Y. Wang, Dynamic nonlinear control for fast seek-settling performance in hard disk drives, *IEEE Trans. on Industrial Electronics*, vol.54, no.2, pp.951-962, 2007.

[5] Q. Hao, R. Chen, G. Guo and S. Chen, A gradient-based track-following controller optimization for hard disk drive, *IEEE Trans. on Industrial Electronics*, vol.50, no.1, pp.108-115, 2003.

[6] Western Digital Technologies, Inc., *Disk Drive Servo Control Technology to Preserve Position Error Signal Continuity During Track Following Operations*, United States Patent US7616399-B1, 2009.

[7] Western Digital Technologies, Inc., *Describes a Method of RRO Learning before and after Shipping to Cancel RRO in a Disk Drive*, United States Patent US6585435-B1, 2003.

[8] S. Kaitwanidvilai and M. Parnichkun, Genetic algorithm based fixed-structure robust H_∞ loop shaping control of a pneumatic servo system, *International Journal of Robotics and Mechatronics*, vol.16, no.4, pp.1716-1725, 2004.

[9] S. Skogestad and I. Postlethwaite, *Multivariable Feedback Control Nd Analysis and Design*, 2nd Edition, John Wiley & Son, NY, USA, 1996.

[10] B. M. Chen, T. H. Lee, K. Peng and V. Venkataramanan, *Hard Disk Drive Servo System*, 2nd Edition, Springer, 2006.

[11] G. F. Franklin, J. D. Powell and A. Emami-Naeini, *Feedback Control of Dynamic Systems*, 3rd Edition, Addison-Wesley, MA, 1994.

[12] L. Dong, H. Zhang, X. Ren and Y.-L. Li, Classifier learning algorithm based on genetic algorithms, *International Journal of Innovative Computing, Information and Control*, vol.6, no.4, pp.1973-1981, 2010.

[13] T.-H. Tan, Y.-F. Huang and F.-T. Liu, Multi-user detection in DS-CDMA systems using a genetic algorithm with redundancy saving strategy, *International Journal of Innovative Computing, Information and Control*, vol.6, no.8, pp.3347-3364, 2010.

[14] C.-H. Chen, T.-Y. Chou, T.-K. Liu, J.-H. Chou and C.-N. Lee, Optimization of short-haul airline crew pairing problems using a multiobjective GA, *International Journal of Innovative Computing, Information and Control*, vol.6, no.9, pp.3943-3959, 2010.

[15] S. Kaitwanidvilai, P. Olarnthichachart and I. Ngamroo, Weight optimization and structure specified robust H infinity loop shaping control of a pneumatic servo system usign genetic algorithm, *International Journal of Robotics and Automation*, vol.25, no.3, 2010.

[16] S. Vachirasricirikul, I. Ngamroo and S. Kaitwanidvilai, Application of electrolyzer system to enhance frequency stabilization effect of micro-turbine in a microgrid system, *International Journal of Hydrogen Energy*, vol.34, no.17, pp.7131-7142, 2010.

[17] A. A. Mamun, G. Guo and C. Bi, *Hard Disk Drive Mechatronics and Control*, CRC Press, 2007.

[18] C. Mohtadi, Bode's integral theorem for discrete-time systems, *IEEE Proc. of Control Theory and Applications*, vol.137, no.2, pp.57-66, 1990.

[19] T. B. Goh, Z. Li, B. M. Chen, T. H. Lee and T. Huang, Design and implementation of a hard disk drive servo system using robust and perfect tracking approach, *IEEE Trans. on Control System Technology*, vol.9, no.2, pp.221-233, 2001.

[20] A. Nath and S. Kaitwanidvilai, High performance HDD servo system using GA based fixed structure robust loop shaping control, *IEEE International Conference on Robotics and Biomimetics*, pp.1854-1859, 2009.

[21] G. Balas, R. Chiang, A. Packard and M. Safonov, *Robust Control Toolbox Getting Started Guide*, 2009.